Submitted to Iron and
Steel International

LBL-1871
c.2

# ROLE OF ELECTRON MICROSCOPY IN DESIGN OF STRONG, TOUGH, ECONOMICAL STRUCTURAL STEELS

Gareth Thomas

August 1973

Prepared for the U.S. Atomic Energy Commission
under Contract W-7405-ENG-48

TWO-WEEK LOAN COPY

*This is a Library Circulating Copy which may be borrowed for two weeks. For a personal retention copy, call Tech. Info. Division, Ext. 5545*

LAWRENCE BERKELEY LABORATORY
UNIVERSITY OF CALIFORNIA
BERKELEY

LBL-1871
c.2

## DISCLAIMER

This document was prepared as an account of work sponsored by the United States Government. While this document is believed to contain correct information, neither the United States Government nor any agency thereof, nor the Regents of the University of California, nor any of their employees, makes any warranty, express or implied, or assumes any legal responsibility for the accuracy, completeness, or usefulness of any information, apparatus, product, or process disclosed, or represents that its use would not infringe privately owned rights. Reference herein to any specific commercial product, process, or service by its trade name, trademark, manufacturer, or otherwise, does not necessarily constitute or imply its endorsement, recommendation, or favoring by the United States Government or any agency thereof, or the Regents of the University of California. The views and opinions of authors expressed herein do not necessarily state or reflect those of the United States Government or any agency thereof or the Regents of the University of California.

# ROLE OF ELECTRON MICROSCOPY IN DESIGN OF STRONG, TOUGH, ECONOMICAL STRUCTURAL STEELS *

Gareth Thomas

Professor of Metallurgy, Department of Materials Science and Engineering, University of California, Berkeley 94720 and Inorganic Materials Research Division, Lawrence Berkeley Laboratory

## ABSTRACT

The microstructures of martensitic and bainitic steels are classified morphologically as determined by thin foil electron microscopy. Correlation of microstructure and properties leads to suggestions for design of strong, tough, economical martensitic and bainitic steels, based on desirable microstructures.

It is shown that as-quenched (autotempered) experimental, vacuum melted, martensitic Fe/Cr/C and Fe/Mo/C steels can have superior mechanical properties to existing and more expensive commercial steels.

It is suggested that lower bainites may be superior to martensites for good mechanical properties in high carbon steels (C > 0.4% C).

---

* Invited paper for "Iron and Steel International"

## I. Background

The overall aim of our present research program is the development of strong, tough, structural steels utilizing martensitic and bainitic transformations as economically as possible. Thus we are concerned with alloys having simplicity of composition and heat treatment, and in which careful attention is paid to control of purity and processing. Alloys are designed so as to ensure for martensitic treatments that there is sufficient hardenability so that no prior decomposition of austenite occurs. The objectives are to design from first principles, desirable microstructures in steels which provide desirable mechanical properties (strength and toughness). Thus the experimental techniques involve detailed metallographic analyses of series of high purity experimental alloys of iron, carbon and one or two substitutional alloying elements such as Cr, Mo, Mn, Ni, Co etc. The microstructures are correlated with the tensile properties and fracture toughness values. The development of fracture mechanics has allowed the determination of a parameter, the plane strain fracture toughness $K_{1c}$ which qualifies as a materials property (e.g. Ref. 1). The complementary applications of modern techniques such as transmission electron microscopy and fracture mechanics has made a major impact on our understanding of the behaviour of materials.

Unfortunately, even since the advent of these techniques, a considerable amount of research has been and still is conducted without taking full advantage of them. Many researchers still conduct mechanical property tests on alloys, but fail to examine the fine microstructures responsible for the properties being measured. On the other hand, in

many alloy systems there are examples of excellent microstructural examinations, but the latter are not correlated quantitatively with appropriate properties e.g. the hardness is quite inadequate to characterize the mechanical properties of steel.

There are, of course, many thorough investigations of both the physical properties and microstructures of alloys, but in most cases, the systems investigated have been commercial alloys. These alloys almost invariably are complicated by the multiplicity of alloying elements and especially by unwanted trace impurities which lead to intergranular embrittlement (2). Since the level of impurities which causes cracking is very low, they cannot be detected metallographically so that sophisticated techniques of spectroscopic analysis such as Auger electron spectroscopy must be employed (2). Even so, heat treatments can be devised which can lead to considerable improvements in the toughness of high strength commercial steels (3).

However, for fundamental studies of the effects of principal alloying elements on the structure and properties of steels it is necessary to use high purity starting materials and vacuum melting techniques, in the preparation of the initial (50 lb) ingots. Details of the experimental methods used in the research program are described elsewhere (e.g. Refs. 4, 5, 11). The program was initiated in 1963 with a systematic approach to the effects of carbon and substitutional elements on the microstructure and mechanical properties of martensitic and bainitic steels. Such investigations, it was hoped, would provide the basis for design of simple steels where the known effects caused by each element can be incorporated into alloys to give a predetermined set of properties.

The research program has been carried out by graduate students leading to post graduate degrees (e.g. Refs. 4 - 12).

The present paper reviews some of our main conclusions from this research program and gives examples of alloys of Fe-C with Cr and Mo which have been designed as a consequence of the program. (Table 1)

In summary, one of the novelties of the research work so far is the fact that it is possible to obtain tough as-quenched martensites in steels containing up to 0.4% C by controlling composition and solution heat treatment. We also know that one can obtain superior properties in lower bainite compared to martensite in higher carbon steels which are normally brittle when untempered after quenching to martensite. The clue for good toughness in all cases has been established from detailed metallographic analysis using high resolution electron microscopy which has identified desirable microstructures. Thus, we believe it is now possible to design the appropriate microstructure for high strength (> 300,000 psi UTS) and toughness properties, without complex compositions or resorting to thermal-mechanical processing. It should be noted of course, that other properties such as fatigue, weldability, corrosion and hydrogen embrittlement susceptibility etc., are not included in this discussion. However, it is emphasized that a basic research program utilizing modern techniques of materials characterization is an essential part of alloy design.

## II. Need for Transmission Electron Microscopy

The primary reason for utilizing transmission electron microscopy is of course its high resolution and the fact that a considerable amount of morphological, crystallographic and other data are obtainable in one

instrument. This is illustrated in the following scheme.

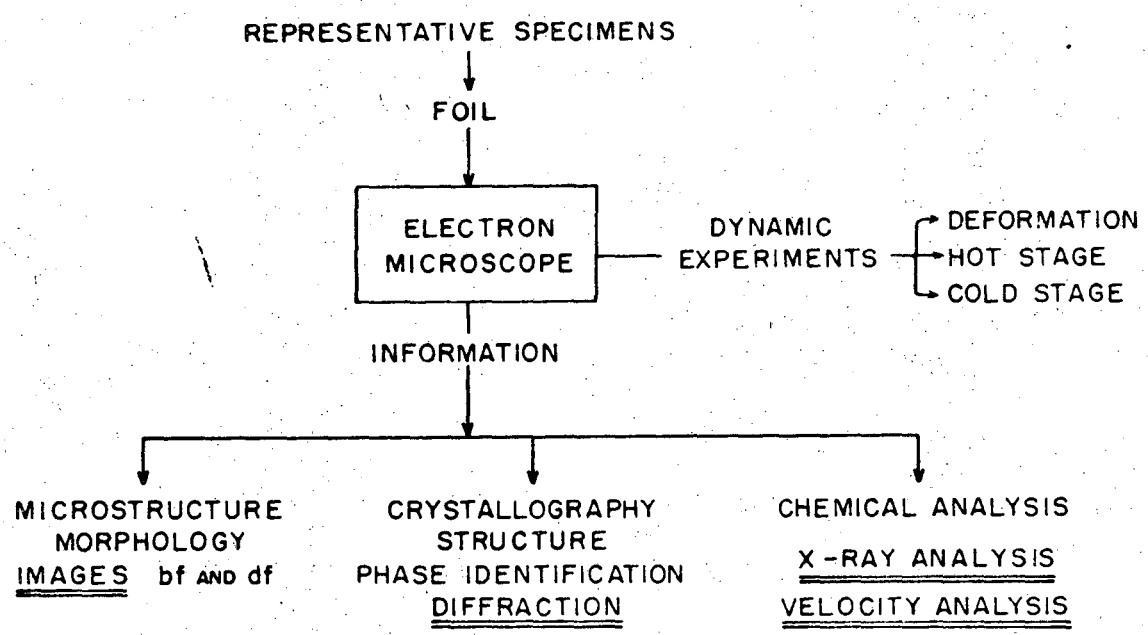


Since the resolution limit of conventional light microscopy is 2000Å and since the carbide particles and substructures of martensite and bainite are generally smaller than this limit (Fig. 1) it is clear that the light microscope cannot distinguish between the possible microconstituents that result from transforming a steel from the austenitic condition. For example by light microscopy one cannot distinguish unequivocally between autotempered martensite and lower bainite after continuous cooling, but one can by electron microscopy because the carbide morphologies and crystallographies are different and can be distinguished. Furthermore, the substructure of the transformation product, which will be termed ferrite in this paper to describe both

martensitic ferrite (with or without dissolved solutes) and bainitic ferrite, is itself complex. In fact martensitic and bainitic ferrites are the most highly deformed structures found in metallurgy.

It should be pointed out that even though the electron microscope can reveal the presence of embrittling microconstituents, only small amounts of material can be examined in each specimen (less than $10^{-6}$ cubic ins). In ultra-high strength steels, only small amounts of austenite decomposition products can lead to embrittlement (e.g. upper bainite). Thus, considerable care and patience must be exercised to ensure that the metallography is properly carried out for representative sampling. It goes without saying that detailed light optical metallography should precede the electron microscopy studies.

Since the morphologies of austenite transformation products are so important in controlling the properties, and because there appears to be some confusion in terminology especially on martensite (e.g. Ref. 13) it will be useful to describe in the following, the representative structures of quenched, tempered, isothermally transformed, or non-pearlitic structural steels, and relate them to strength and toughness properties.

## III. Microstructures of Martensitic and Bainitic Steels

### (a) As-Quenched Martensite

Provided steel has sufficient hardenability to avoid any decomposition of austenite prior to transformation to martensite, the microstructure consists either of dislocated laths, twinned plates or both (13). The principal features are illustrated in Fig. 2. The micro-twinning in martensite is distinguished by contrast experiments and analysis of selected area diffraction patterns (4, 7, 14). The first papers dealing

with the microstructure of martensite were those of Kelly and Nutting (14) who showed that increasing carbon and nickel and subsequent lowering of $M_s$ temperature increased the probability of transformation twinning. Subsequent work on the effects of other alloying elements, including cobalt, which does not have much influence on $M_s$ temperature, has shown that all of the principal alloying elements C, Ni, Mn, Cr, Mo, Co increase the tendency to twinning (4, 5, 8, 11, 12). It has been suggested by Thomas (6) that the transformation structure depends on the relative values of the critical resolved shear stresses for slip and twinning over the $M_s$-$M_f$ transformation range as illustrated in Fig. 3. Thus, the lower the $M_s$-$M_f$ temperatures and the stronger the steel then the inhomogeneous shear component of the transformation strain will be twinning rather than slip.

If the $M_s$ temperature is kept at about 300°C or higher the structure is principally dislocated. However, on quenching, autotempering can occur and although the strength is lowered, the toughness is usually better. As Fig. 4 shows, carbon has the strongest influence on $M_s$ temperature and so 0.4% carbon is the upper limit if large amounts of twinning are to be avoided. This result confirms the initial work on binary Fe-C alloys by Kelly and Nutting (14).

Although increasing carbon increases the strength and hardness of martensite, (see summary in Fig. 5) the toughness drops dramatically. This is illustrated from a series of Fe-Ni-Co-C alloys (4) with carbon ranging from 0.2 to 0.4% in Fig. 6. The important result from this work is that, as shown in Fig. 6, <u>at the same strength level</u> the twinned

martensite has a lower fracture toughness than the dislocated martensite.

Although it may be argued that it is really the carbon content and not the twinning that is responsible for this phenomenon, recent work on Fe-Cr-C steels (11) has clearly shown that in as-quenched steels, for the same carbon content, fracture toughness decreases with increasing twinning. This is illustrated in Fig. 7. Since Cr is known not to be a solid solution strengthener, we believe it is now clearly established that (internal) transformation twinning, whilst increasing strength (Figs. 5, 7) seriously impairs toughness in the presence of carbon. It should be noted from Fig. 7 that the 4% Cr steels have excellent $K_{1c}$ toughness properties even in the process untempered condition (11).

Likewise in Fig. 9, toughness decreases for increasing % Mn at the same carbon level (0.24%C) after treatment to produce similar strength levels (5). The steels designated 804-806 contain 5% nickel also whereas steels 807-809 have no nickel. For increasing manganese contents, the amount of twinning after quenching to martensite increases and the toughness deteriorates. At 7% Mn the martensites are almost entirely twinned (5). Fig. 10 shows a summary for a series of Fe-Cr-C steels (11).

The martensite transformation is perhaps the most efficient way of generating uniformly, very dense dislocation configurations (Fig. 2A). The only other way such microstructures can be generated is by very high strain-rate plastic deformation such as shock loading. For example, in fcc metals a critical shock pressure exists beyond which mechanical twinning becomes the mode of deformation, Fig. 8a (15). Furthermore, there is a discontinuous increase in hardness as shown in Fig. 8b. Thus, by analogy to these results we can conclude that internal twinning itself

increases the strength of metals and in steels it is additive to the strengthening from carbon in solution. This is schematically indicated by the shaded area in Fig. 5. The fall-off in hardness above about 0.7%C is due to the fact that the $M_s$ temperature drops so much (Fig. 4) it is impossible to obtain 100% martensite. Thus, because of these factors, it is dangerous to use hardness as a measure of carbon content for steels containing more than about 0.3% carbon.

In conclusion, therefore, it can be seen that to obtain high toughness the problem in designing martensitic alloys is to avoid twinning. Since carbon has the most dramatic effect on lowering $M_s$, (Fig. 4) we believe 0.4% carbon (in solution) represents the maximum possible carbon content. The simple ternary Fe-4Cr-0.35C steel and Fe-2Mo-0.4C steel (Table 1) even in the as-quenched martensitic condition have been designed to meet this requirement. As can be seen in Figs. 7 and 11, the Fe-4Cr-0.35C alloy (0435 designation in Fig. 11) has properties equal or superior to existing more complex (and more expensive) commercial steels. An obvious possible application for this new steel includes aircraft landing gear (compare to 4340 and 300M which are currently in use).

"As-quenched" and "tempered" are two major descriptive terms for martensite which were originally process-oriented. The expression "as-quenched" has been used so widely to be differentiated from the name "tempered", consequently an ambuiguity is generated. That is, when the term "as-quenched" martensite is used it refers to the diffusionless martensitic transformation product without subsequent carbide precipitation. This pure as-quenched martensite is generally associated with poor mechanical properties and is the one avoided in the steel-making

industry.

However, autotempering usually takes place in the as-quenched martensite of the developmental steels, e.g. Fe-Cr-C and Fe-Mo-C (See Fig. 12F). Superior mechanical properties are obtained in the as-quenched martensite of these experimental alloys which violates the traditional rule "as-quenched steels are poor". In order to eliminate this contradiction, it seems to be appropriate now to establish the expressions of "process as-quenched" or "process untempered" and "structurely as-quenched" or "structurely untempered" which clearly identifies the product structure after particular heat treatment. Besides, if autotempering is involved during the quenching treatment, it is best to describe this explicitly as "autotempered as-quenched martensite" to distinguish it from the conventional "as-quenched martensite". Therefore, "structurely untempered" martensites such as an extensively twinned one (high carbon and other solutes and low $M_s$-$M_f$) which has poor mechanical properties are to be shunned. In order to achieve some autotempering the $M_s$-$M_f$ range cannot be too low. Consequently an $M_s$ near 350°C should be aimed at; as Fig. 4 shows it is possible to calculate the total alloy content to meet this requirement.

Furthermore, the amount of autotempering depends on the cooling rate (which is also affected by the size of the specimen) as well as on the composition of the alloy investigated. The excellent mechanical properties of the process as-quenched martensite of the experimental Fe-Cr-C and Fe-Mo-C alloys (Table 1) may partly be related to autotempering. Thus, by optimizing the amount of autotempering through controlled cooling rate and alloy content together with the imposition of other design criteria, a superior martensitic steel with simple heat treatment can be developed, even in 0.4% carbon steels.

A special effect has been observed in our work on Fe-Cr-C steels which delays the precipitation of interlath carbides. This effect is the existence of extremely narrow films of retained austenite around the martensite laths. These films are difficult to analyze and require patient studies by selected area electron diffraction. Not only may these films contribute to the high toughness of the as-quenched Fe-4Cr-C martensites, but they delay the precipitation of embrittling interlath carbides up to 400°C which represents reasonable tempering resistance. It is not yet established whether or not the presence (and quantity) of interlath austenite is a prerequisite for high toughness in as-quenched martensitic alloys,* although clearly such austenite should impede microcrack growth.

A further point which research has brought out is the benefit resulting from using higher austenitizing temperatures (11). For Fe-Cr-C and Fe-Mo-C steels it is necessary to austenitize at 1100°C or a little higher so as to dissolve all carbides. Again light microscopy is inadequate to determine this and thin foil electron microscopy is necessary. Undissolved carbides can cause cracking during the $\gamma \rightarrow \alpha$ martensitic transformation especially if the carbides are non-coherent and cannot deform with the matrix. The volume increase on the $\gamma \rightarrow \alpha$ transformation could also produce voids or cracks around undissolved carbides. Zackay et al. (3) have also found a pronounced effect on toughness in a secondary hardening Fe-5%Mo-0.3%C and in 4130 and 4340 commercial steels by austenitizing above 1100°C. The latter effect may be related to desegregation of impurities at grain boundaries, and/or increasing the amount of inter-lath austenite(3).

(b) Process Tempered Martensite

Tempering martensite produces precipitation of cementite ($Fe_3C$)

* In stainless steels retained austenite clearly improves toughness (D. Webster, Met. Trans. 2, 2097 (1971).

and other carbides. The morphology depends upon the martensitic substructure, the composition and tempering temperature, and Figs. 12E-K show typical examples. In the absence of secondary hardening (hardening due to precipitation of alloy carbides such as molybdenum carbides), the tempering range which produces interlath carbides should be avoided (Fig. 12G) because the toughness deteriorates and intergranular embrittlement occurs (4,5). This effect is similar to that in Al-Zn-Mg alloys (aged to peak hardness). In general, tempering produces a lowering of strength and an increase in toughness as a result of precipitation of iron carbide, for example in Fig. 11 the Fe-4Cr-0.35C steel at point T. Characterization of these complex structures requires repeated application of dark field techniques as is illustrated in the micrographs of Figs. 2, 12 and 13.

(c) Isothermal Transformations - Bainites

If metastable austenite in a low alloy steel is held at a temperature above $M_s$, it will decompose isothermally into a product of deformed ferrite and carbide called bainite which closely resembles the structure of tempered martensite. Two generally distinct morphologies known as upper (high temperatures) and lower (low temperatures) bainite occur. Typical examples are shown in Fig. 13. The upper bainite is not of much technical interest since the interlath carbides cause embrittlement, and thus decomposition of austenite to upper bainite must be avoided. Continuous cooling through the lower bainite range could be an economical way of producing lower bainite.

Lower bainite has potential for high strength and toughness at higher carbon levels than seems feasible for martensites. The relative

differences between toughness of lower bainite vs tempered martensite have been discussed in terms of the differences in carbide morphologies and matrix substructures (10). In fact, high carbon Fe-Ni-Co-C alloys show higher toughness and strength when transformed to lower bainite than after quenching to martensite and then tempered (4). This can be seen from the circled region in Fig. 11. The toughness of martensitic 9Ni-4Co-0.45C at similar strength levels is about one-third of the values shown in Fig. 11 (ref. 4 and data of Republic steel).

The transformation mechanism of austenite to bainite has been a topic of argument for many years. The precipitation process, especially the initial stage, in the bainitic transformation, is not thoroughly understood. The characterization of the nature and the crystallography of carbide phases are important in order to understand the structural features of bainite (16). It is generally accepted that cementite $Fe_3C$ constitutes the carbide phase in upper bainite. Although cementite is frequently observed in lower bainite, the exact carbide precipitation process is still uncertain. It has been suggested by Oblak and Heheman (17) that epsilon carbide is the first carbide formed in low temperature bainite. Since the carbide precipitation in steel may assume many different forms such as epsilon carbide, Hägg carbide, cementite, etc., depending on the transformation temperature and time, as well as composition of the steel, the characterization of carbide must be approached with great care. Unfortunately, it is frequently not possible to unambiguously determine the nature of the carbides present because of competing factors and their complex structures.

In order to try to understand these complexities, we are currently

investigating the nature of bainite in a wide range of alloys (differing composition and transformation temperature (18). The results indicate that except for twinning, lower bainite has all of the features known for tempered dislocated martensites. For example an Fe-0.54C-1.87Si steel with $M_s$ of 250°C, after isothermal transformation to lower bainite at 275°C consists of a high density of epsilon carbide precipitates uniformly distributed throughout the bainitic ferrite matrix. The crystallographic relationship between the epsilon carbide and the bainitic ferrite is found to follow that of Jack's orientation relationship[19]. i.e., $(0001)_\varepsilon \parallel (011)_\alpha$ and $(10\bar{1}1)_\varepsilon \parallel (101)_\alpha$.

The unambiguous identification of the existence of epsilon-carbide in lower bainite further supports the view that the transformation mechanism by which lower bainite forms initially as supersaturated ferrite from which epsilon-carbide precipitates very rapidly and is subsequently replaced by cementite upon further transformation. Also, it is evident that the nature of the carbide phase that exists in lower bainitic structures depends on the transformation temperature and time as well as on the composition of the steel under investigation. Also contrary to some researchers (16) we have found that characteristic lower bainitic structures can be observed in some steels transformed above 350°C. This means that 350°C is <u>not</u> an invariant temperature which defines an upper-lower bainite transition.

## IV. Summary and Conclusions

The principal metallographic features of martensites, tempered martensites and bainites can be resolved and distinguished by thin film transmission electron microscopy. There are summarized in Table 2.

Desirable microstructures from the point of view of good fracture resistance are dislocated martensitic/bainitic lath ferrites, autotempered martensite, interlath films of retained austenite, tempered martensite free from interlath carbides, and lower bainite. Thus, in order to obtain high strength and toughness, the following basic rules for controlling microstructure apply:

(a) As-quenched Martensites:

Austenitize at 1100°C or higher to take all carbides into solution; avoid transformation twinning by controlling carbon and keep $M_s$ above about 300°C. This determines total alloy content permissable (e.g. Fig. 4). For dislocated martensites the strength depends on carbon content: to avoid twinning $\%C \leq 0.4\%$ Ternary alloying additions provide desired properties e.g. hardenability in order to prevent prior austenite decomposition to upper bainite, examples Fe-4Cr-0.35C, and Fe-2Mo-0.4C and correspond to steels with $M_s \approx 320°C$. Some autotempering during the cooling below $M_s$ may be beneficial to toughness. Also the presence of interlath retained austenite is beneficial for high toughness.

(b) Tempered Martensites:

Toughness drops when interlath carbides precipitate; these may be delayed from forming by allowing fine films of retained austenite to remain around the martensite laths (low additions of Ni, Mn, or Co may facilitate this).

(c) Bainites:

Upper bainite should be avoided at all cost. Lower bainite is similar to tempered martensite but does not usually contain interlath

carbides. This structure is desirable for high toughness and thus lower bainite could give attractive properties in high carbon steels (C > 0.4%). This can be achieved economically if 100% lower bainite can be formed on continuous cooling from the austenitizing temperature. Knowledge of CCT diagrams are thus essential.

## V. Acknowledgments

I wish to thank the U.S. Atomic Energy Commission through the Inorganic Materials Research Laboratory for continued financial support of this program. I acknowledge also the gifts of alloys from Republic Steel, and Ford Motor Company, and innumerable helpful discussions with my students especially D. Huang, Drs. S. J. Matas and F. A. Hultgren (Republic Steel) and the continued encouragement and stimuli provided by Professors V. F. Zackay and E. R. Parker.

Table 1

Examples of Room Temperature

Mechanical Properties of Vacuum Melted Experimental Steels

A. Fe-Cr-C Series[11]

| Alloy | Treatment | 0.2% offset Yield Strength (psi) | UTS (psi) | % el. | Plane Strain Fracture Toughness $K_{1c}$ KSI-in$^{1/2}$ |
|---|---|---|---|---|---|
| 4Cr-0.17C | As-quenched[a] | 160,000 | 194,000 | 10 | 83 |
| | Temp 200°C 1 hr | 166,000 | 195,000 | 9.5 | 92 |
| | " 400°C " | 162,000 | 185,000 | 9.7 | 83 |
| | " 600°C " | 91,000 | 106,000 | 15.0 | * |
| 4Cr-0.35C | As-quenched[a] | 240,000 | 306,000 | 5 | 70 |
| | Temp 200°C 1 hr | 218,000 | 275,000 | 7.5 | 92 |
| | " 400°C " | 201,000 | 237,000 | 9.0 | 77 |
| | " 600°C " | 126,000 | 149,000 | 17.0 | * |

*Not determinable - even 1 ins thick specimens gave invalid $K_{1c}$ data due to very high toughness (note high elongations)

B. Fe-Mo-C Series[12]

| | | | | | |
|---|---|---|---|---|---|
| 3.85Mo-0.18C | As-quenched[a] | 160,000 | 198,000 | 12.6 | 93 |
| | Temp 400°C 1 hr | 153,000 | 183,000 | 14 | 89 |
| | " 600°C " [b] | 193,000 | 205,000 | 8.5 | 46 |
| 2.2Mo-0.4C | As-quenched[a] | 258,000 | 311,000 | 2.5 | 54 |
| | Temp 400°C 1 hr | 197,000 | 230,000 | 5.8 | 94 |
| | " 600°C " | 206,000 | 223,000 | 10.7 | 73 |

(a) 100% Martensite

(b) Secondary hardening - precipitation of $Mo_2C$

Table 2

Summary of microstructures of martensitic and bainite steels.*

| Constituent | Notes | Structure |
|---|---|---|
| Martensite (as-quenched) | $C \leq 0.4$ $Ms \geq 300°C$ | Dislocated laths; if autotempered Widmanstatten {110} cementite |
| | $C \geq 0.4$ $Ms \leq 200°C$ | {112} and {110} (high C) twinned plates; carbides on twins |
| Tempered Martensite | Dislocated Martensite | Epsilon carbide with {100} habit precipitates initially and is replaced by three variants of {110} Widmanstatten cementite as the tempering temperature is increased. Alloy carbides can form at higher temperatures, or longer tempering times. |
| | Twinned Martensite | Single carbide variants on twin boundaries; as above. |
| Lower Bainite | | Dislocated ferrite with single variant $Fe_3C$ oriented 55-65° to lath; no interlath carbides so far no clear cut evidence for twinned ferrite; epsilon carbide possible. |
| Upper Bainite | | Dislocated ferrite; interlath carbides. No unique transition temperature for lower to upper bainite transformation--depends on composition. |

* Mixtures of all of these constituents are possible depending on composition and transformation kinetics.

## References


1. Fracture Toughness of High Strength Materials: Theory and Practice, Iron & Steel Inst. Special Publication No. 120, London, 1970.
2. McMahon, C. J. Jr., "Temper Embrittlement in Steel" STP No. 407 ASTM Philadelphia, 1968, p 127.
3. Zackay, V. F., Parker, E. R. and Wood, W. E., "Influence of Some Microstructural Features on the Fracture Toughness of High Strength Steels", Third Int. Conf. on Strength of Metals and Alloys, Cambridge, England, Inst. of Metals, London, 1973, 1 pp. 175-179.
4. Das, S. K. and Thomas, G., "Structure and Mechanical Properties of Fe-Ni-Co-C Steels", Trans. ASM, 62, 1969, p 659.
5. Huang, D. H. and Thomas, G., "Structure and Mechanical Properties of Tempered Martensite and Lower Bainite in Fe-Ni-Mn-C Steels", Met. Trans. 2, 1971, 1587-1598.
6. Thomas, G., "Electron Microscopy Investigations of Ferrous Martensites", Met. Trans. 2, 1971, 2373.
7. Thomas, G. and Das, S. K., "Multiple Transformation Twinning in Ferrous Martensites", J. of the Iron & Steel Institute, 209, 1971, p 801.
8. Raghavan, M. and Thomas, G., "Structure and Mechanical Properties of Fe-Cr-C-Co Steels", Met. Trans. 2, 1971, 3433-3439.
9. Cheng, I-Lin and Thomas G., "The Enhancement of Strengthening Dislocated Martensite", Met. Trans. 3, 1972, 503-516.
10. Huang, D. H. and Thomas, G., Author's Reply to the Discussion of: "Structure and Mechanical Properties of Tempered Martensite and Lower Bainite in Fe-Ni-Mn-C Steels", Met. Trans., 3, No. 1, 1972, pp 343-346.

11. McMahon, J. and Thomas, G., "Development of Strong, Tough, Economical Fe-Cr-C Steels", Third Int. Conf. on Strength of Metals and Alloys, "Microstructure and Design of Alloys", Cambridge, England, 1973, 1, pp 180-184.

12. Clark, R. A. and Thomas, G., Met. Trans., to be published.

13. e.g., "Physical Properties of Martensite and Bainite", ISI Report No. 93, Iron & Steel Inst., London, 1965 and Symposium on Martensite, Met. Trans., 2, 1971 pp 2326-2462.

14. Kelly, P. M. and Nutting, J., Proc. Royal Soc. A259, 1960 p 45: "Physical Properties of Martensite and Bainite", ISI Report No. 93, Iron and Steel Inst., London 1965, p 166.

15. Nolder, R. L. and Thomas, G., Acta Met. 12, 1964, p 191.

16. Shackleton, D. N. and Kelly, P. M., ISI Special Report No. 93, Iron and Steel Inst., London, 1965, p 126.

17. Oblak, J. M. and Heheman, R. F., Transformation and Hardenability in Steels, Climax Molybdenum Company, 1967, p 15.

18. Huang, D. H. and Thomas, G., Reported at AIME Spring Meeting, Philadelphia, Pa., 1973, to be published.

19. Jack, K. H., JISI, 169, 1951, pp 26-36.

## FIGURE CAPTIONS

Fig. 1. A. Light microscope photograph of martensite in as-quenched Fe-Ni-Co alloy. B. Transmission electron micrograph of same specimen as A showing that the grain structure actually consists of bundles of densely dislocated martensite laths. Courtesy Trans ASM 61, 14 (1968).

Fig. 2a. Bright field image of as-quenched martensite in Fe-25Ni-10Co steel. The dislocated lath structure is typical of low carbon martensites and yields high toughness with moderate to high tensile strength. b) shows the bright field image of a twinned martensite plate in Fe-28.5Ni-10Co steel. c) is a related dark field image of twin reflection. The corresponding selected area diffraction pattern is shown in d), and indicates the dark field image is formed by superimposed twin and matrix reflections. The complexity of the substructure, with matrix dislocations and multiple twinning, is revealed by this technique. Twinned martensite normally occurs when carbon content exceeds approximately 0.3% or in general when the total solute content increases. Except for cobalt, increasing the solute content also lowers the $M_s$ temperature. The presence of a high twin density in a martensitic structural steel has been found to be associated with low fracture toughness and high yield strength.

Fig. 3. Scheme showing relationship between substructure of martensite (inhomogeneous shear), and transformation temperature. The levels will be affected by the concentration of solutes (which affects the yield strength of martensite) as indicated by arrows. Courtesy Met. Trans. ( Ref. 6).

Fig. 4. Scheme (not to scale) showing effects of alloying elements on the $M_s$ temperature of binary Fe based steels. The numbers give the drop in °C per wt % solute. The dotted line indicates the approximate lower level of $M_s$ temperature above which autotempering is to be expected. Extensive twinning is expected in carbon bearing steels when $M_s < 200°C$.

Fig. 5. Showing effect of carbon on hardness of binary Fe-C martensites (after Kelly and Nutting Ref. 14). On the diagram is also shown schematically some of the structural and strength contributions as a function of % carbon.

Fig. 6. Showing the relationship between yield strength and fracture toughness for a series of Fe-Ni-Co-C steels. Notice at the same yield stress the dislocated martensite is tougher than the twinned martensite as shown by the bright field images (twins marked T) (Ref. 4, courtesy Amer. Soc. Met.).

Fig. 7. Showing relationship between as-quenched yield strength, plane strain fracture toughness and relative fraction of internally twinned martensite for experimental Fe-Cr-C steels. (Ref. 11).

Fig. 8. a) Nickel after shock loading to 350kb pressure showing substructure of dense dislocations and mechanical twins on two {111} planes; notice similarity to martensitic substructure (Fig. 2).

b) Hardness of nickel as a function of shock loading; notice discontinuity when twinning sets in. Courtesy Acta Met., Ref. 15.

Fig. 9. Showing effect of % manganese on impact energy at various yield strengths of a series of quenched and tempered martensitic steels

containing 0.24%C. Steels 804-806 contain 5%Ni, steels 807-809 have no nickel. Courtesy Met. Trans. Ref 5.

Fig. 10. Summary of yield strength vs fracture toughness for a series of quenched, and quenched and tempered Fe-Cr-C steels containing 0.17C and 0.35%C (see Fig. 7). Courtesy J. McMahon.

Fig. 11. Comparison of ultimate tensile strengths and fracture toughness of the experimental Fe-4Cr-0.35C steel (Ref. 11) with similar properties in some commercial steels (latter data courtesy R. Ault, G. Waid and R. Bertolo, Tech. Rep AFML-TR-71-27).

Fig. 12. Dark field imaging is an essential technique for determining the distribution and orientation of carbide precipitates in tempered martensites. (E) is a dark field image of a carbide reflection in Fe-9 Ni-4 Co-0.45C steel tempered at 500°F for 4 hours, showing the precipitation of epsilon carbide on {100} martensite planes. The initial formation of $Fe_3C$ on {110} martensite planes is seen at A. Epsilon carbide will precipitate only at low tempering temperatures and dissolves upon formation of $Fe_3C$ at higher temperatures. (F) illustrates the dark field image of a Widmanstatten pattern of $Fe_3C$ in Fe-4Cr-5.3Co-0.35C tempered at 400°F for 4 hours. This precipitate substructure is found in almost all dislocated martensites tempered at low temperatures, as well as in as-quenched martensites which undergo autotempering due to their high $M_s$ temperatures. The formation of a Widmanstatten pattern of $Fe_3C$ is accompanied by "normal" tempering behavior, viz., an increase in fracture toughness and a decrease in yield strength. At higher tempering temperatures, carbides may precipitate along martensite

lath boundaries, causing a marked decrease in toughness. (G) shows a dark field image of interlath carbides in the same alloy as in (F) tempered at 800°F for 4 hours. At very high tempering temperatures, the carbides spherodize producing an increase in toughness and a further reduction in yield strength. A dark field image of spherodized carbides is shown in (H), which is the same steel as in (F) tempered at 1000°F for 4 hours. When twinned martensites are tempered, the carbides precipitate along the twin boundaries. The twin boundary carbides have been associated with a decrease in fracture toughness in structural steels. (I) is a bright field image of a twinned martensite plate in Fe-27Ni-10Co-0.1C steel, where the twin density is highest at the midrib. The steel was tempered at 200°C for 1 hour, and a Widmanstatten pattern of $Fe_3C$ is seen outside the twinned area. (J) shows a dark field image of the twins, and (K) is a dark field image of the unidirectional carbides on the twin boundaries. Note that the particular $Fe_3C$ reflection used in (K) illuminates only the twin boundary carbides and not the Widmanstatten pattern outside the twinned area. This points out the need for imaging several different carbide reflections in order to determine completely the precipitate morphology. These examples illustrate that the tempering behaviour depends on the initial martensitic substructure which can vary within each plate as well as from plate (or lath) to plate.

Fig. 13. (L) is the bright field image of upper bainite in Fe-4Cr-0.34C steel, and (M) is the dark field image of a carbide reflection, showing the characteristic elongated carbides between the bainitic

ferrite laths. Upper bainite, which is formed at high isothermal transformation temperatures, normally has a low fracture toughness. Note the similarity of the carbide morphology in (M) with that shown in 12(G), a tempered martensite which is likewise embrittled by interlath carbides. At lower transformation temperatures, the $Fe_3C$ precipitates unidirectionally within the bainite laths. This is seen in (N), the bright field image of lower bainite in Fe-4Cr-5.3Co-0.35C steel. The dark field image in (O) reverses the contrast of the carbides. Normally the carbides in lower bainite form at an angle of 55° to 65° to the long direction of the bainite laths. The carbide morphology of lower bainite in (L) and (M) is similar to that of dislocated martensite tempered at low temperatures, as seen in (12E,F). Both structures also exhibit high toughness values. It is thus seen that by comparing upper bainite with tempered martensite having interlath carbides, and lower bainite with tempered martensite having Widmanstatten carbides, there is a strong correlation between microstructure and mechanical properties. In steels having a twinned martensitic substructure and poor toughness, it may be preferable to utilize isothermal transformations to produce dislocated lower bainite having a higher toughness due to the similarity of its structure with that of tempered dislocated martensite.

IM 2473 Upper Left

Fig. 1A

IM2473 Upper Right

Fig. 1B

Class 4

DISLOCATED AND TWINNED AS-QUENCHED MARTENSITES

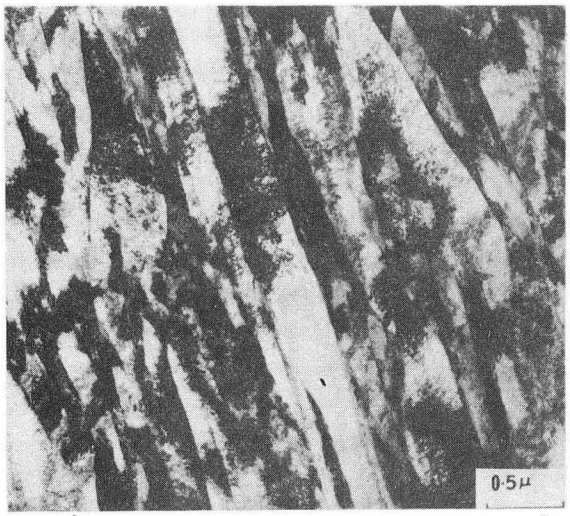


Magnification: 45,000X

A

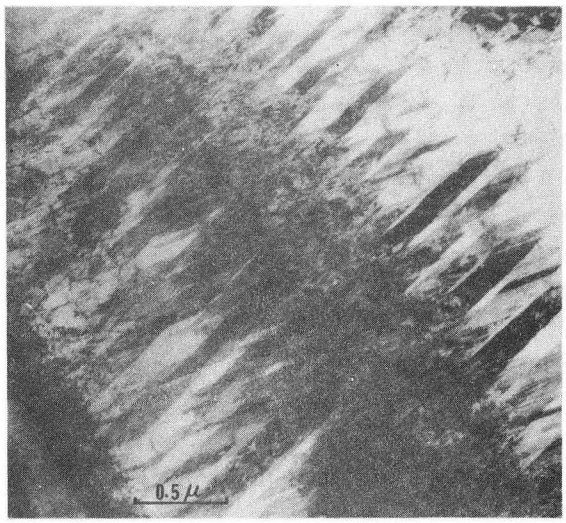


B

Magnification: 56,000X

(A) is a bright field image of as-quenched martensite in Fe-25 Ni-10 Co steel. The dislocated lath structure is typical of low carbon martensites and yields high toughness with moderate to high tensile strength. (B) shows the bright field image of a twinned martensite plate in Fe-28.5 Ni-10 Co steel. (C) is a related dark field image of a twin reflection. The corresponding selected area diffraction pattern is shown in (D), and indicates the dark field image is formed by superimposed twin and matrix reflections. The complexity of the substructure, with matrix dislocations and multiple twinning, is revealed by this technique. Twinned martensite normally occurs when carbon content exceeds approximately 0.3% or in general when the total solute content increases. Except for cobalt, increasing the solute content also lowers the Ms temperature. The presence of a high twin density in a martensitic structural steel has been found to be associated with low fracture toughness and high yield strength.

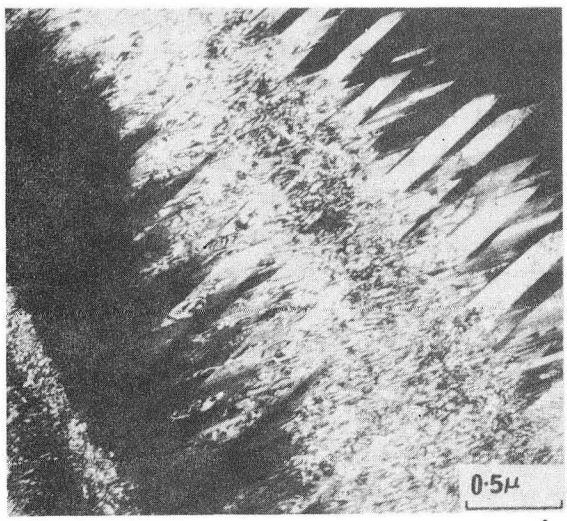


Magnification: 56,000X

C

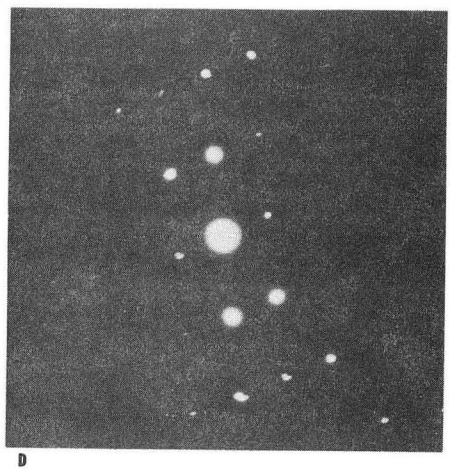

D

XBB 729-4502

Fig. 2

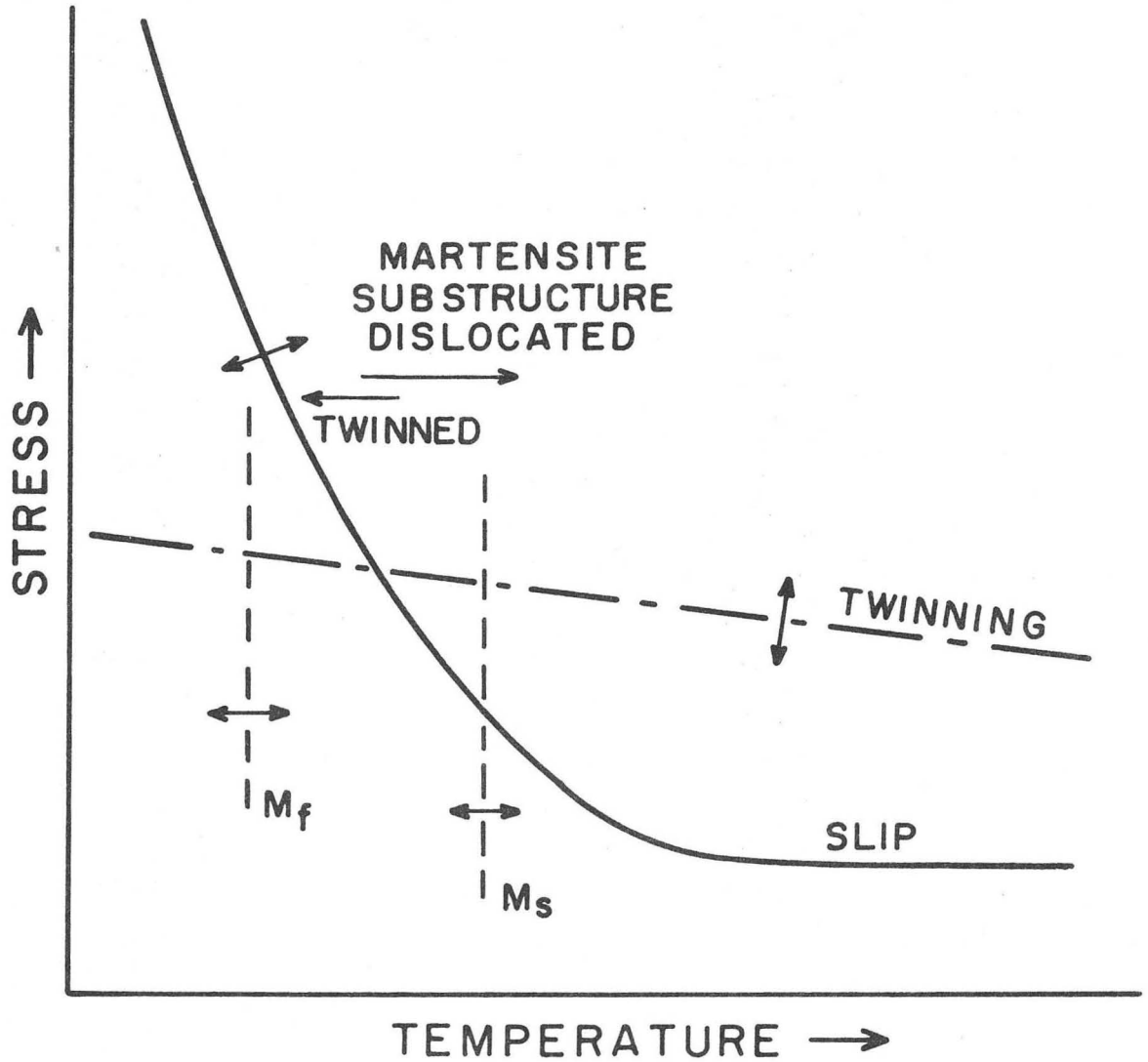


XBL 705-890

Fig. 3

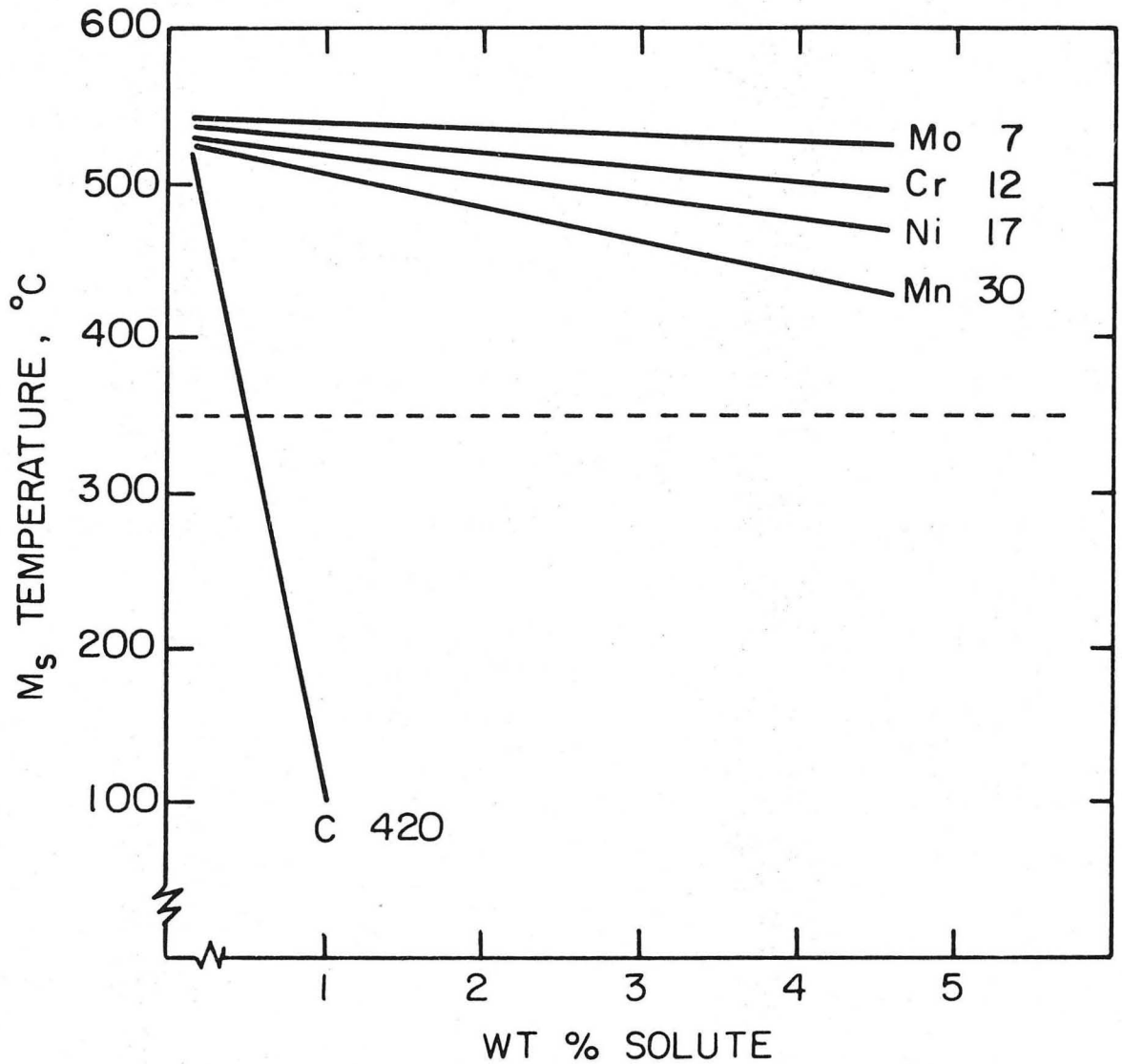


SCHEMATIC DRAWING (NOT TO PROPORTION) OF THE EFFECT OF ALLOYING ELEMENTS ON $M_s$ TEMPERATURE OF STEEL

XBL 7212-7361

Fig. 4

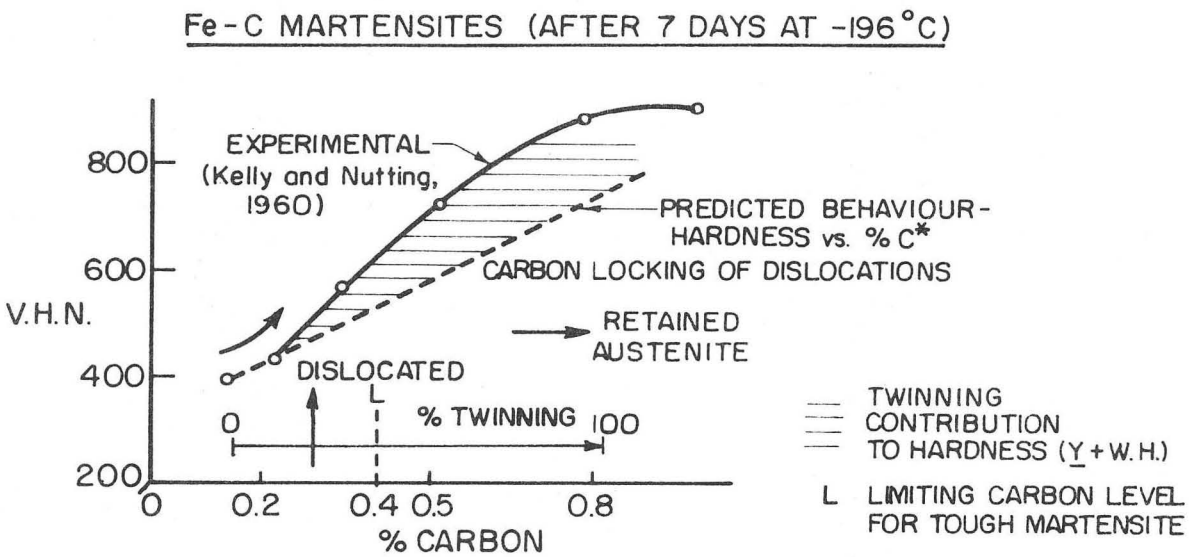


XBL 7211-7195

Fig. 5

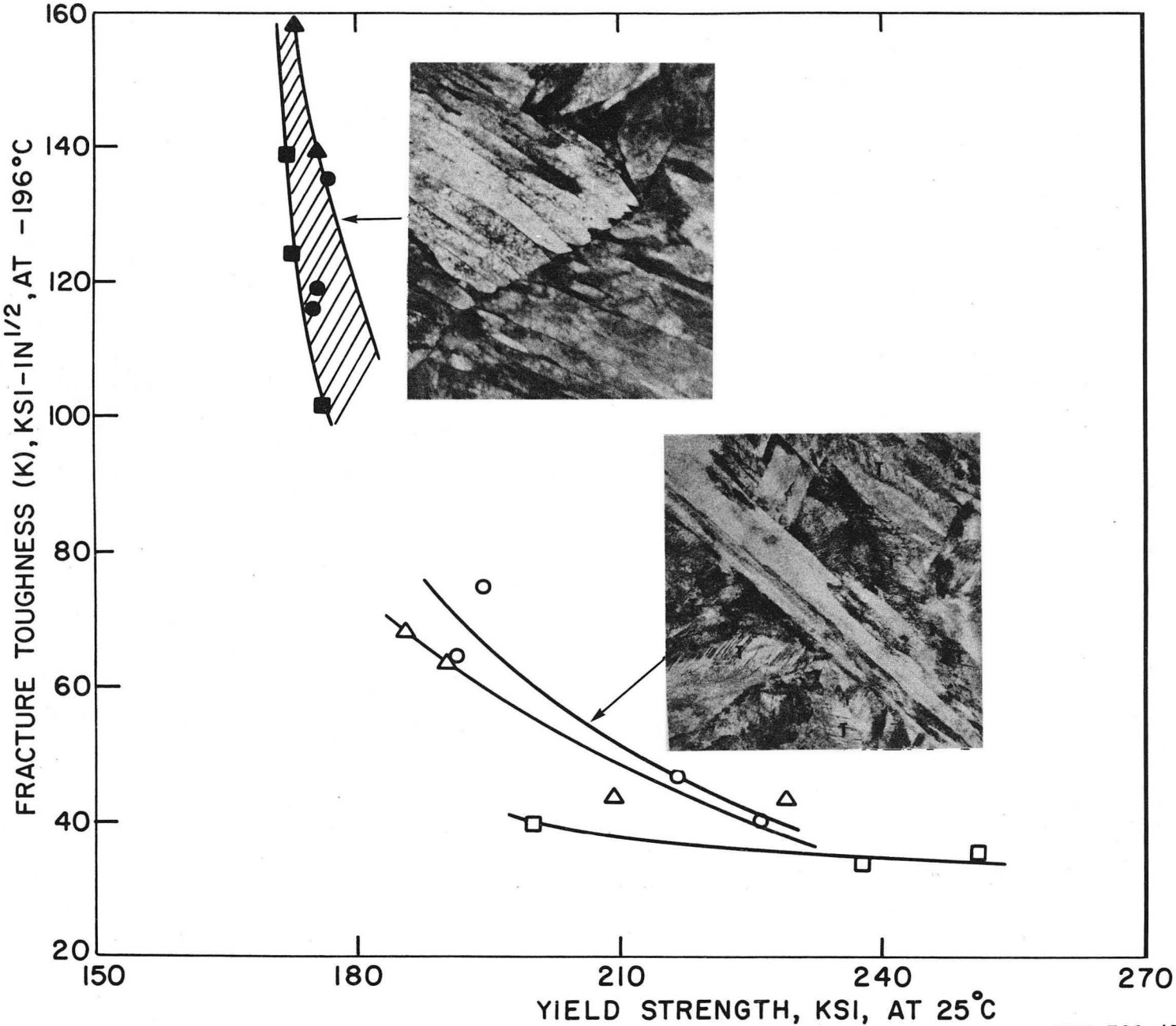


XBB 701-475

Fig. 6

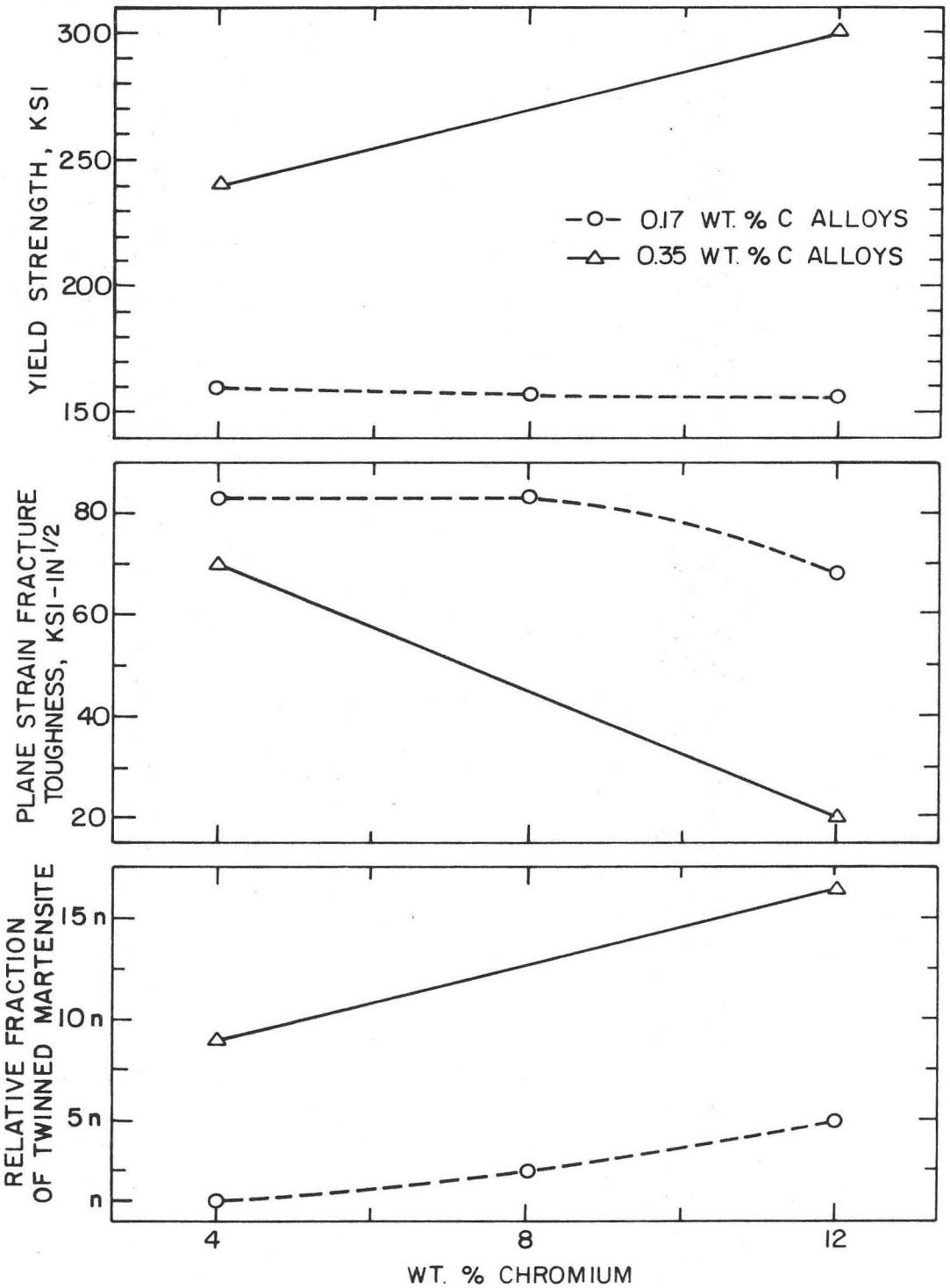


XBL 7211-7156

Fig. 7

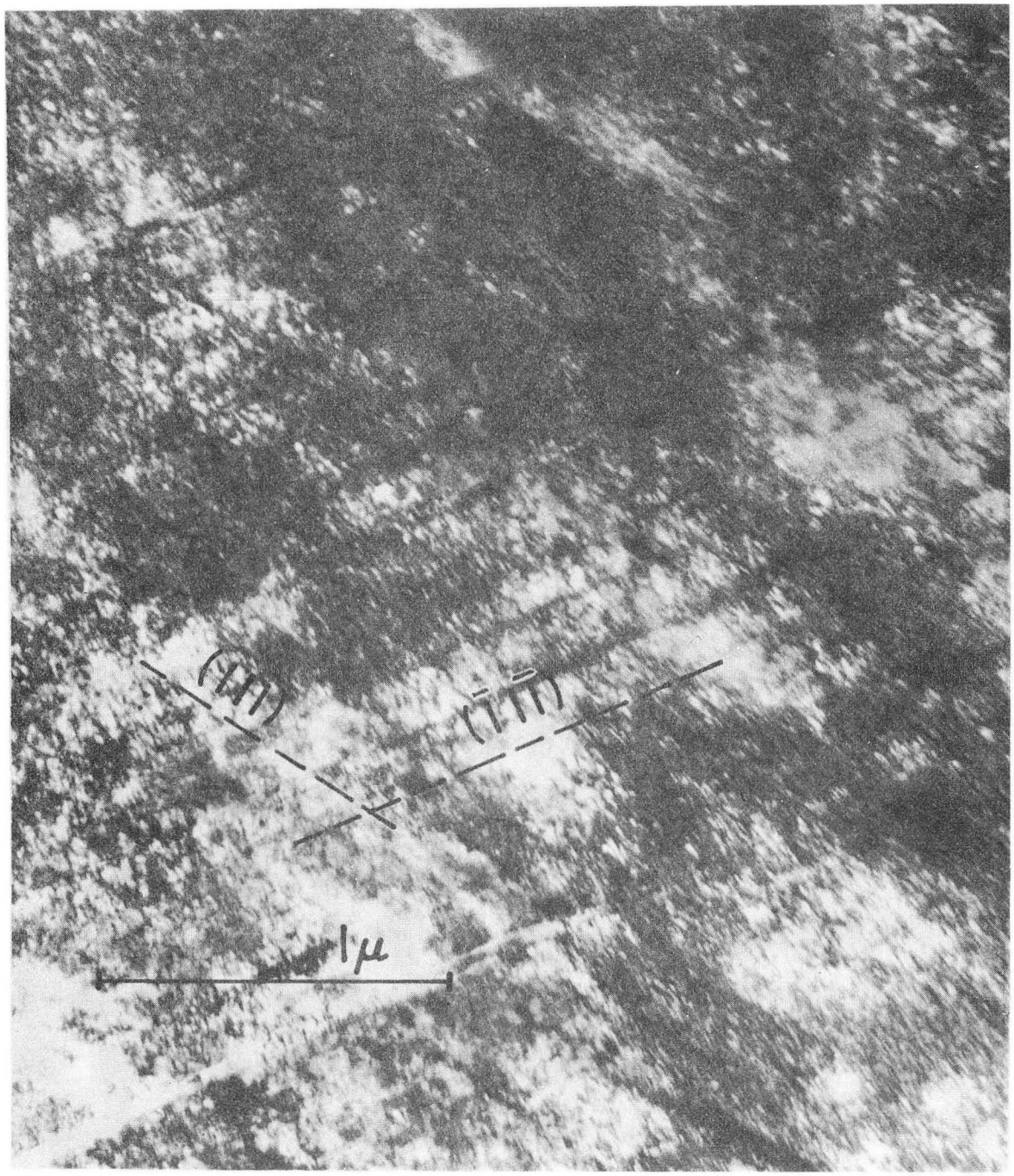


IM 983 A Only

Fig. 8 A

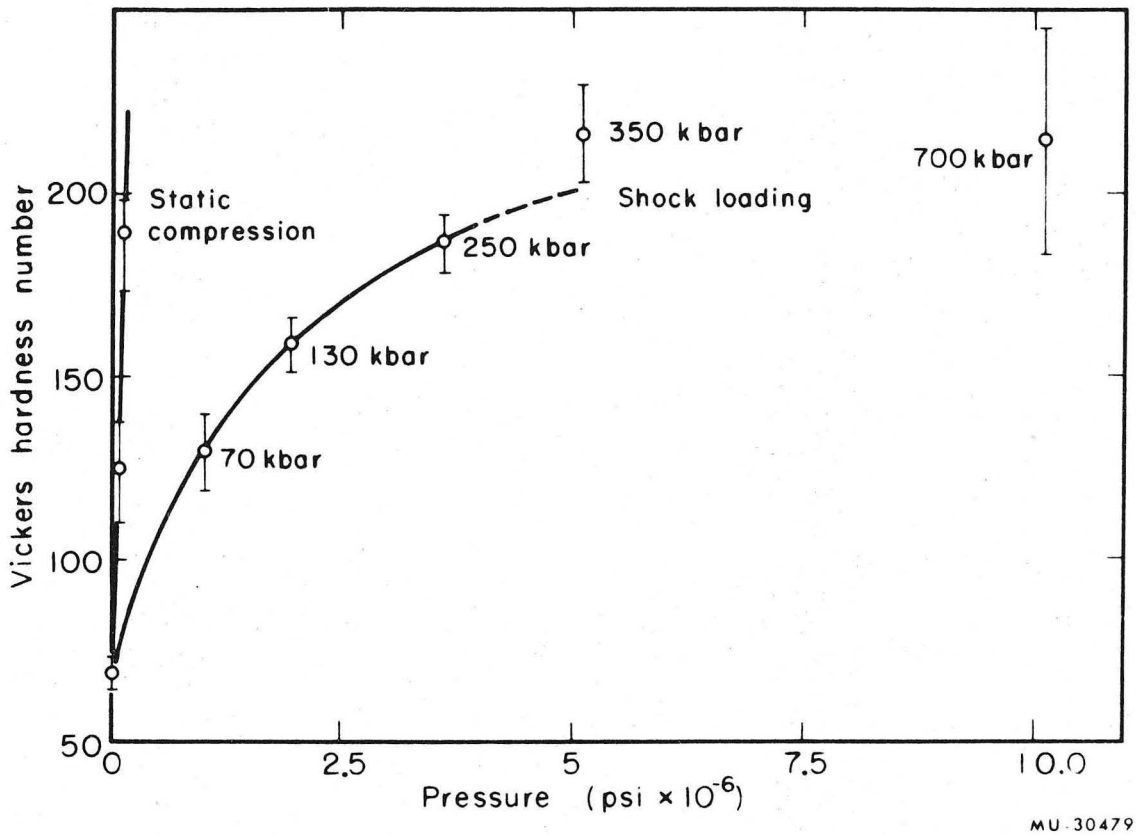
Vickers hardness number
200
150
100
50
0
2.5
5
7.5
10.0
Pressure (psi × 10^-6)
Static compression
350 k bar
Shock loading
700 k bar
250 kbar
130 kbar
70 kbar
MU-30479

Fig. 8B

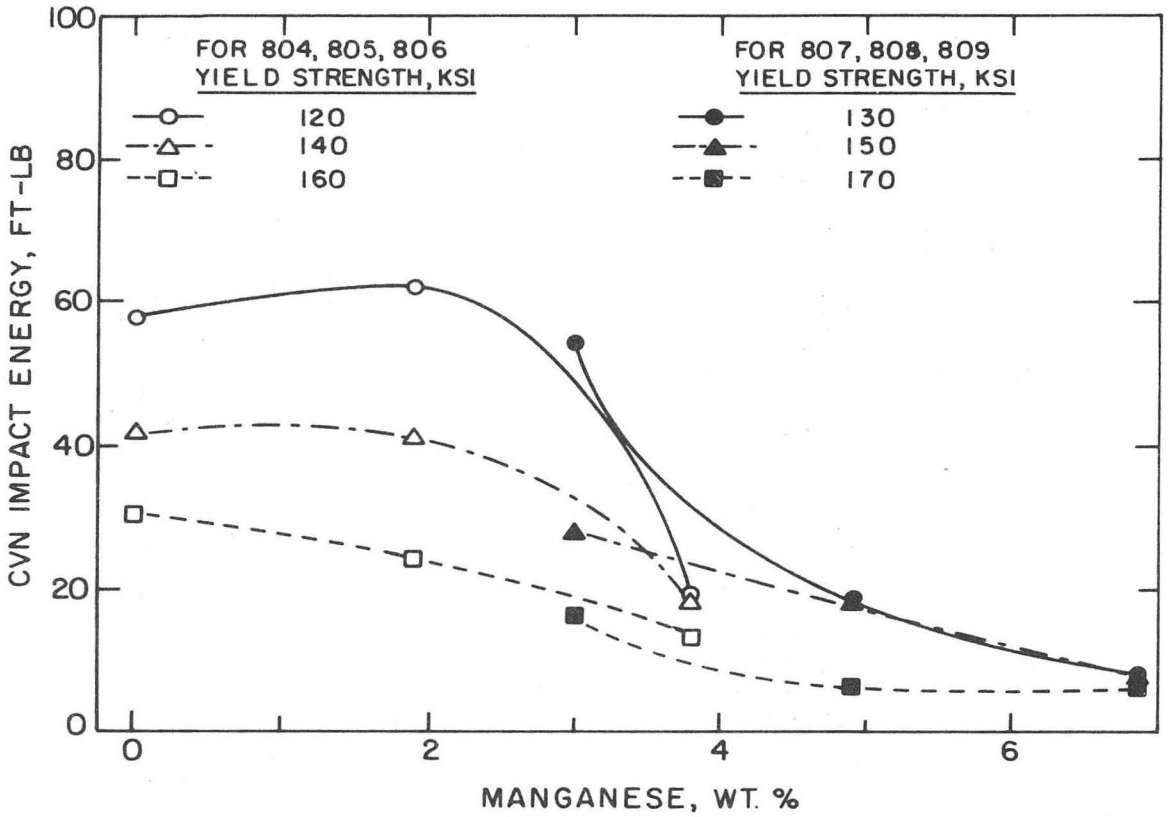


XBL 708-1707

Fig. 9

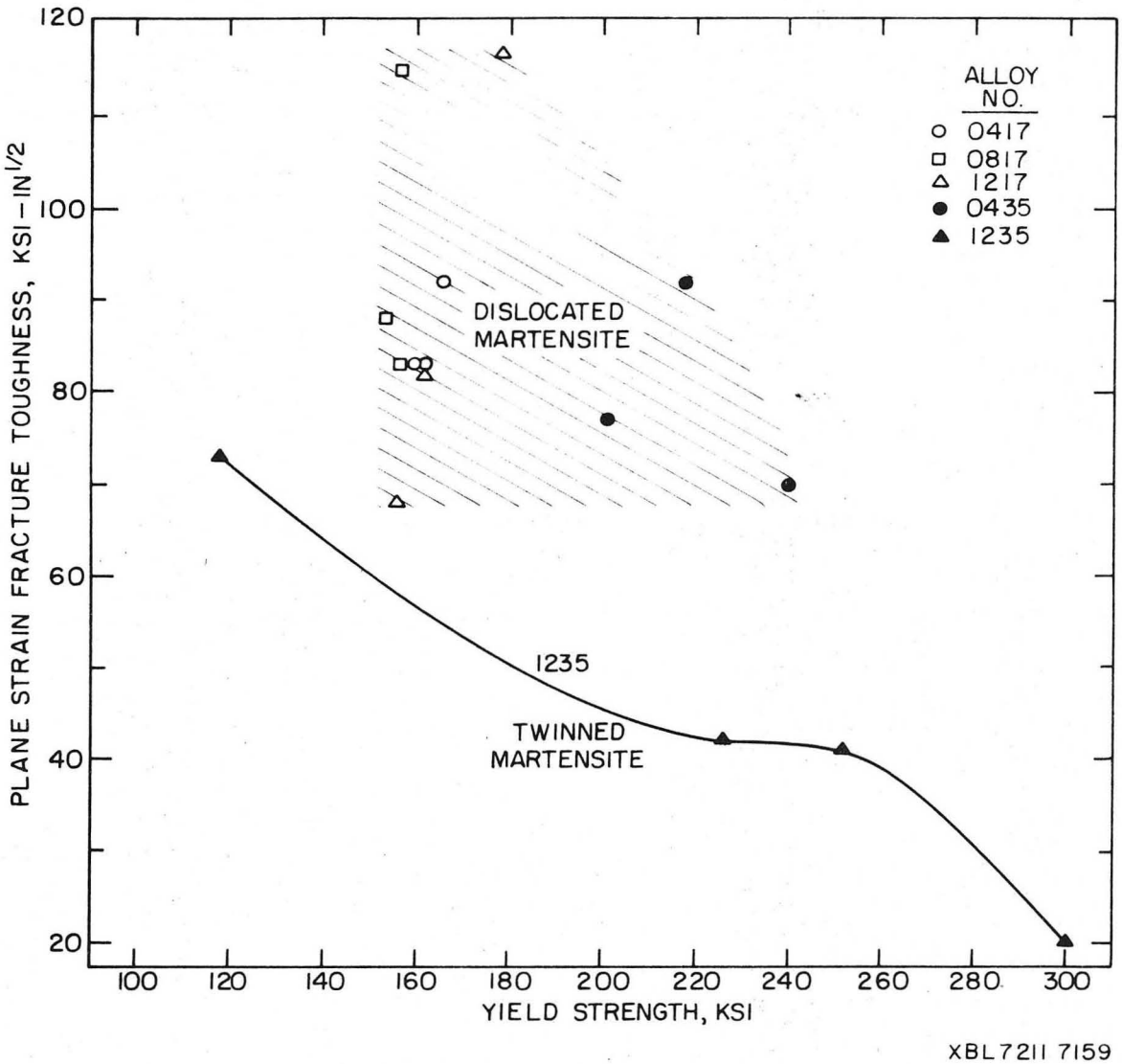
120
100
80
60
40
20
PLANE STRAIN FRACTURE TOUGHNESS, KSI-IN$^{1/2}$
100
120
140
160
180
200
220
240
260
280
300
YIELD STRENGTH, KSI
ALLOY NO.
0417
0817
1217
0435
1235
DISLOCATED MARTENSITE
1235
TWINNED MARTENSITE
XBL7211 7159

Fig. 10

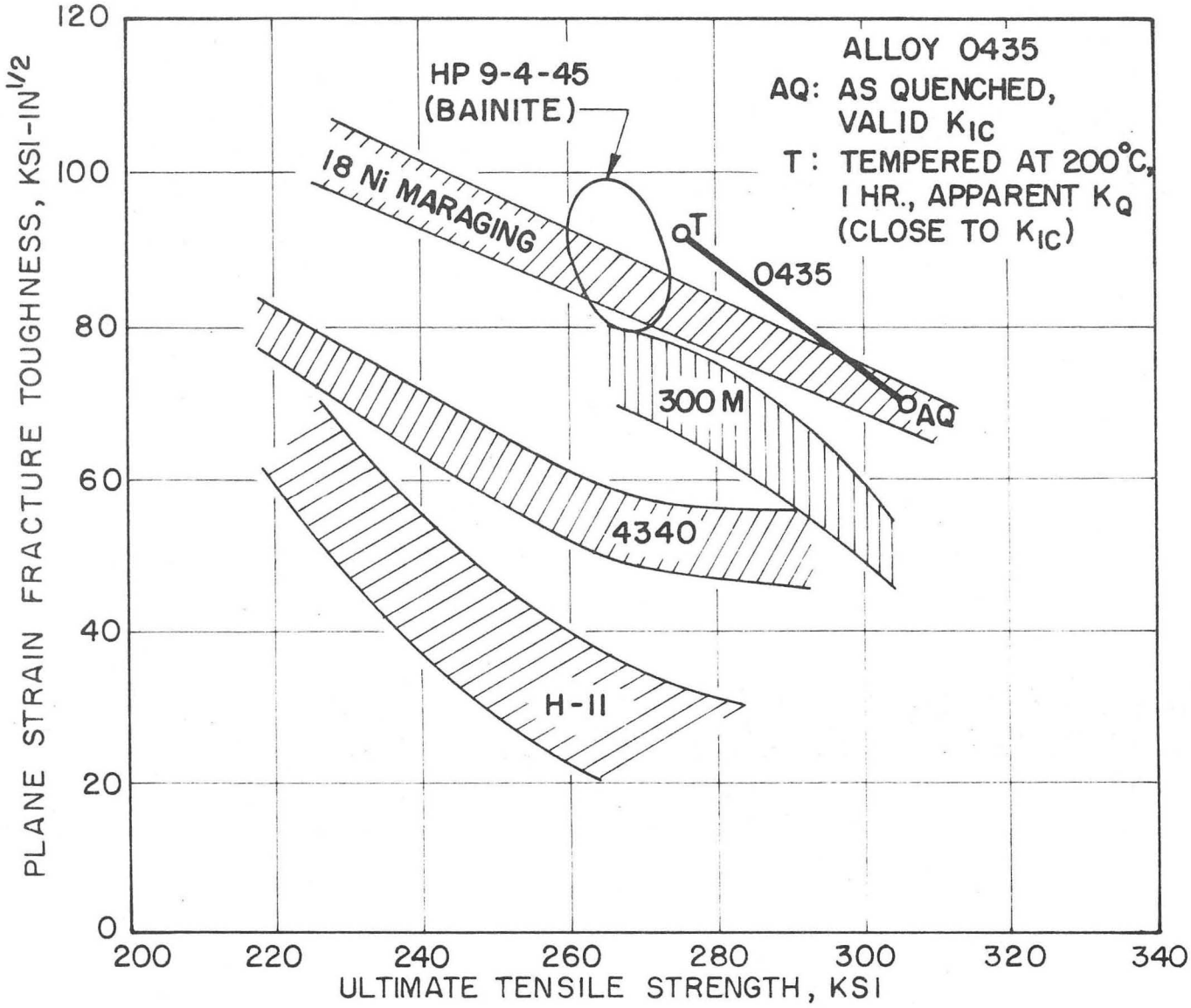


XBL7211-7161

Fig. 11

Class 4

# TEMPERED DISLOCATED MARTENSITE

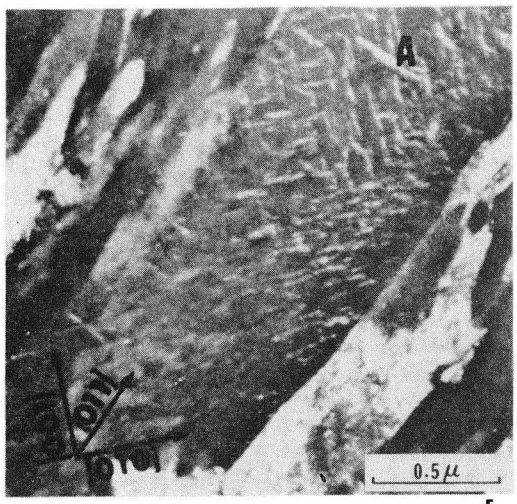


Magnification: 76,000X

E

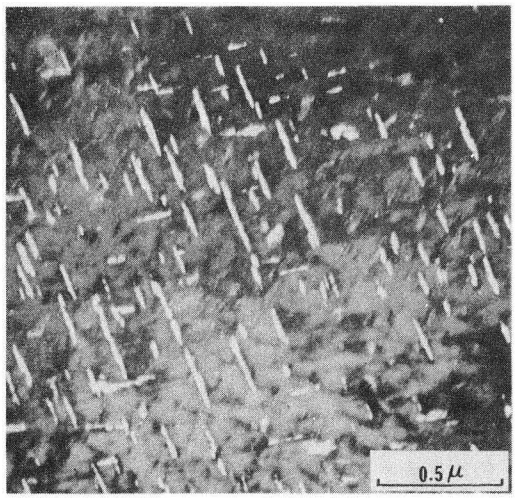


F

Magnification: 75,000X

Dark field imaging is an essential technique for determining the distribution and orientation of carbide precipitates in tempered martensites. (E) is the dark field image of a carbide reflection in Fe-9 Ni-4 Co-0.45 C steel tempered at 400 °F for 4 hours, showing the precipitation of epsilon carbide on {100} martensite planes. The initial formation of $Fe_3C$ on {110} martensite planes is seen at A. Epsilon carbide will precipitate only at low tempering temperatures and dissolves upon formation of $Fe_3C$ at higher temperatures. (F) illustrates the dark field image of a Widmanstatten pattern of $Fe_3C$ in Fe-4Cr-5.3 Co-0.35C tempered at 400 °F for 4 hours. This precipitate substructure is found in almost all dislocated martensites tempered at low temperatures, as well as in as-quenched martensites which undergo autotempering due to their high Ms temperatures. The formation of a Widmanstatten pattern of $Fe_3C$ is accompanied by "normal" tempering behavior, viz, an increase in fracture toughness and a decrease in yield strength.

At higher tempering temperatures, carbides may precipitate along martensite lath boundaries, causing a marked decrease in toughness. (G) shows a dark field image of interlath carbides in the same alloy as in (F) tempered at 800° F for 4 hours. At very high tempering temperatures, the carbides spherodize producing an increase in toughness and a further reduction in yield strength. A dark field image of spherodized carbides is shown in (H), which is the same steel as in (F) tempered at 1000° F for 4 hours.

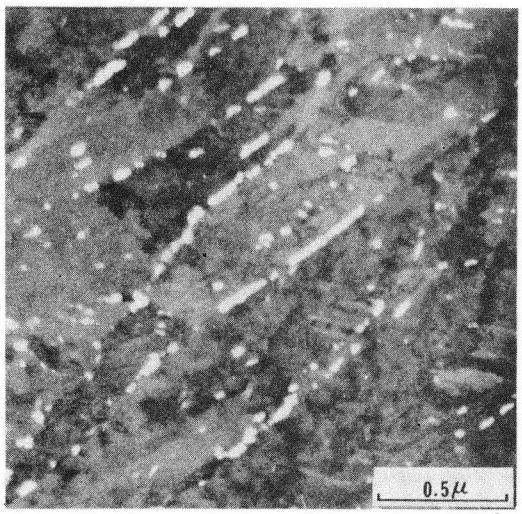


Magnification: 77,000X

G

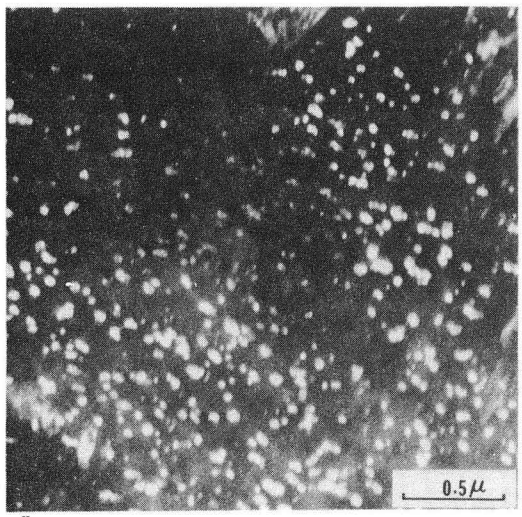


H

Magnification: 60,000X

XBB 729-4504

Fig. 12

Class 4

# TEMPERED TWINNED MARTENSITE

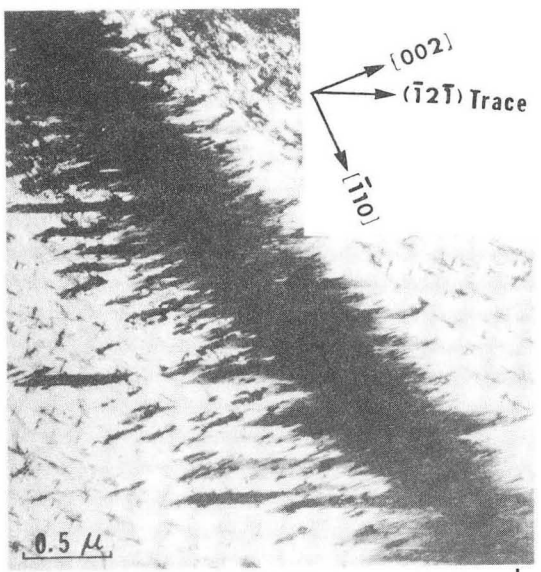


Magnification: 52,000X

I

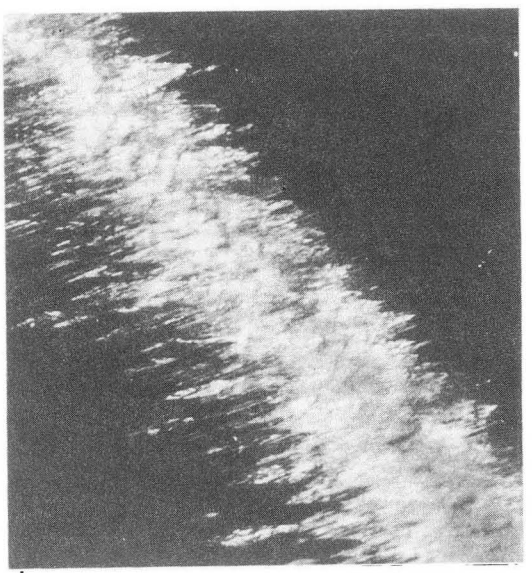

J

Magnification: 52,000X

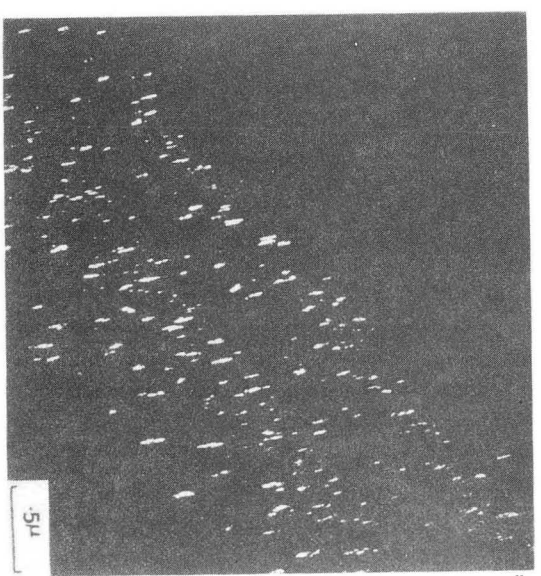


Magnification: 52,000X

K

When twinned martensites are tempered, the carbides precipitate along the twin boundaries. The twin boundary carbides have been associated with a decrease in fracture toughness in structural steels. (I) is the bright field image of a twinned martensite plate in Fe-27 Ni-10 Co-0.1C steel, where the twin density is highest at the midrib. The steel was tempered at 200° C for 1 hour, and a Widmanstatten pattern of $Fe_3C$ is seen outside the twinned area. (J) shows a dark field image of the twins, and (K) is a dark field image of the unidirectional carbides on the twin boundaries. Note that the particular $Fe_3C$ reflection used in (K) illuminates only the twin boundary carbides and not the Widmanstatten pattern outside the twinned area. This points out the need for imaging of several different carbide reflections in order to determine completely the precipitate morphology. These examples illustrate that the tempering behavior depends on the initial martensitic substructure which can vary within each plate as well as from plate (or lath) to plate.

XBB 729-4505

Fig. 12 cont.

Class 4

# ISOTHERMAL TRANSFORMATIONS

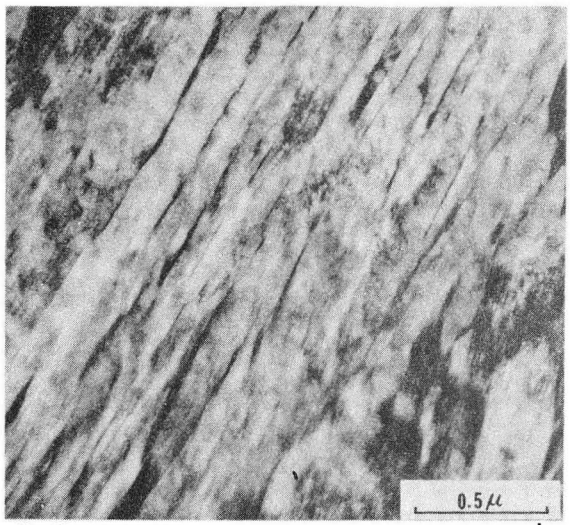


Magnification: 80,000X

L

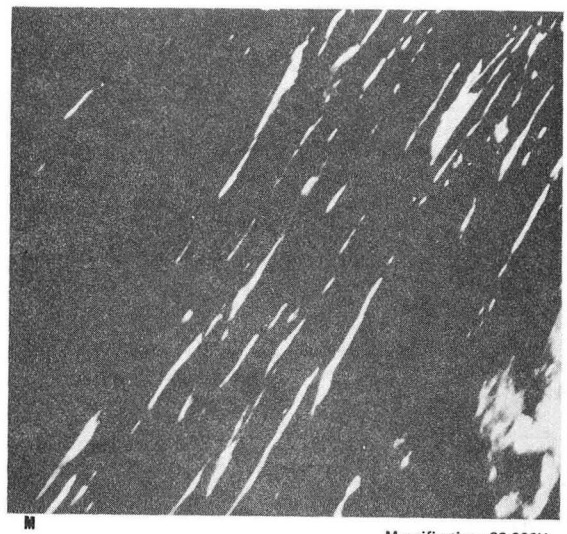

M

Magnification: 80,000X

(L) is the bright field image of upper bainite in Fe-4Cr-0.34 C steel, and (M) is the dark field image of a carbide reflection, showing the characteristic elongated carbides between the bainitic ferrite laths. Upper bainite, which is formed at high isothermal transformation temperatures, normally has a low fracture toughness. Note the similarity of the carbide morphology in (M) with that shown in (G), a tempered martensite which is likewise embrittled by interlath carbides.

At lower transformation temperatures, the $Fe_3C$ precipitates unidirectionally within the bainite laths. This is seen in (N), the bright field image of lower bainite in Fe-4Cr-5.3Co-0.35C steel. The dark field image in (O) reverses the contrast of the carbides. Normally the carbides in lower bainite form at an angle of 55° to 65° to the long direction of the bainite laths. The carbide morphology of lower bainite in (L) and (M) is similar to that of dislocated martensite tempered at low temperatures, as seen in (E) and (F). Both structures also exhibit high toughness values. It is thus seen that by comparing upper bainite with tempered martensite having interlath carbides, and lower bainite with tempered martensite having Widmanstatten carbides, there is a strong correlation between microstructure and mechanical properties.

In steels having a twinned martensitic substructure and poor toughness, it may be preferable to utilize isothermal transformations to produce dislocated lower bainite having a higher toughness due to the similarity of its structure with that of tempered dislocated martensite.

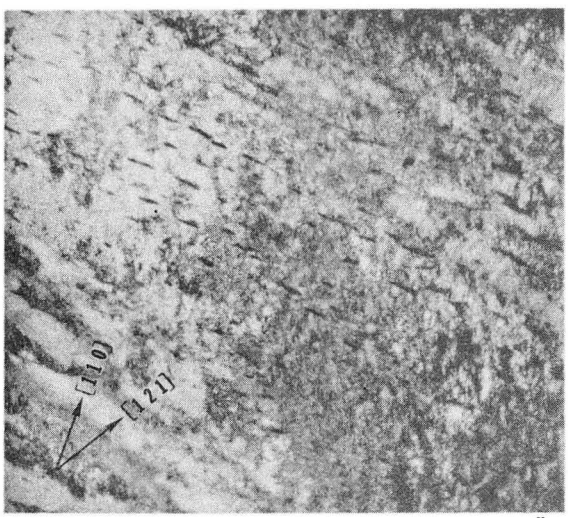


Magnification: 80,000X

N

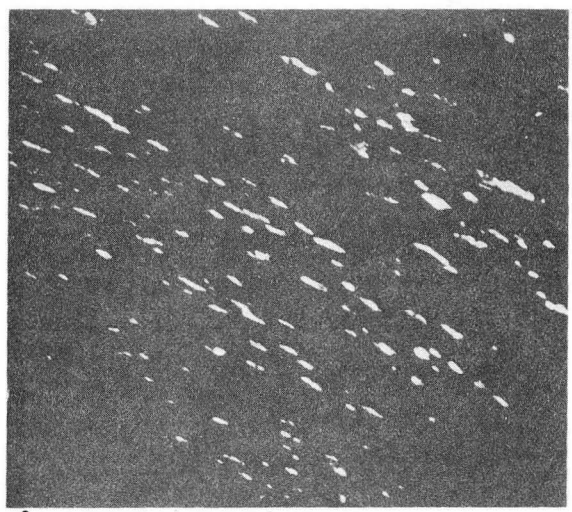

O

Magnification: 80,000X

XBB 729-4503

Fig. 13

LEGAL NOTICE

*This report was prepared as an account of work sponsored by the United States Government. Neither the United States nor the United States Atomic Energy Commission, nor any of their employees, nor any of their contractors, subcontractors, or their employees, makes any warranty, express or implied, or assumes any legal liability or responsibility for the accuracy, completeness or usefulness of any information, apparatus, product or process disclosed, or represents that its use would not infringe privately owned rights.*

*TECHNICAL INFORMATION DIVISION*
*LAWRENCE BERKELEY LABORATORY*
*UNIVERSITY OF CALIFORNIA*
*BERKELEY, CALIFORNIA 94720*